BABAR-PUB-01/19
SLAC-PUB-9102

Search for the Rare Decays $B \to K \ell^+ \ell^-$ and $B \to K^* \ell^+ \ell^-$

B. Aubert,[1] D. Boutigny,[1] J.-M. Gaillard,[1] A. Hicheur,[1] Y. Karyotakis,[1] J. P. Lees,[1] P. Robbe,[1] V. Tisserand,[1]
A. Palano,[2] A. Pompili,[2] G. P. Chen,[3] J. C. Chen,[3] N. D. Qi,[3] G. Rong,[3] P. Wang,[3] Y. S. Zhu,[3] G. Eigen,[4]
B. Stugu,[4] G. S. Abrams,[5] A. W. Borgland,[5] A. B. Breon,[5] D. N. Brown,[5] J. Button-Shafer,[5] R. N. Cahn,[5]
A. R. Clark,[5] M. S. Gill,[5] A. V. Gritsan,[5] Y. Groysman,[5] R. G. Jacobsen,[5] R. W. Kadel,[5] J. Kadyk,[5] L. T. Kerth,[5]
Yu. G. Kolomensky,[5] J. F. Kral,[5] C. LeClerc,[5] M. E. Levi,[5] G. Lynch,[5] P. J. Oddone,[5] M. Pripstein,[5] N. A. Roe,[5]
A. Romosan,[5] M. T. Ronan,[5] V. G. Shelkov,[5] A. V. Telnov,[5] W. A. Wenzel,[5] T. J. Harrison,[6] C. M. Hawkes,[6]
D. J. Knowles,[6] S. W. O'Neale,[6] R. C. Penny,[6] A. T. Watson,[6] N. K. Watson,[6] T. Deppermann,[7] K. Goetzen,[7]
H. Koch,[7] M. Kunze,[7] B. Lewandowski,[7] K. Peters,[7] H. Schmuecker,[7] M. Steinke,[7] N. R. Barlow,[8] W. Bhimji,[8]
N. Chevalier,[8] P. J. Clark,[8] W. N. Cottingham,[8] B. Foster,[8] C. Mackay,[8] F. F. Wilson,[8] K. Abe,[9] C. Hearty,[9]
T. S. Mattison,[9] J. A. McKenna,[9] D. Thiessen,[9] S. Jolly,[10] A. K. McKemey,[10] V. E. Blinov,[11] A. D. Bukin,[11]
D. A. Bukin,[11] A. R. Buzykaev,[11] V. B. Golubev,[11] V. N. Ivanchenko,[11] A. A. Korol,[11] E. A. Kravchenko,[11]
A. P. Onuchin,[11] S. I. Serednyakov,[11] Yu. I. Skovpen,[11] V. I. Telnov,[11] A. N. Yushkov,[11] D. Best,[12] M. Chao,[12]
D. Kirkby,[12] A. J. Lankford,[12] M. Mandelkern,[12] S. McMahon,[12] D. P. Stoker,[12] K. Arisaka,[13] C. Buchanan,[13]
S. Chun,[13] D. B. MacFarlane,[14] S. Prell,[14] Sh. Rahatlou,[14] G. Raven,[14] V. Sharma,[14] C. Campagnari,[15]
B. Dahmes,[15] P. A. Hart,[15] N. Kuznetsova,[15] S. L. Levy,[15] O. Long,[15] A. Lu,[15] J. D. Richman,[15] W. Verkerke,[15]
J. Beringer,[16] A. M. Eisner,[16] M. Grothe,[16] C. A. Heusch,[16] W. S. Lockman,[16] T. Pulliam,[16] T. Schalk,[16]
R. E. Schmitz,[16] B. A. Schumm,[16] A. Seiden,[16] M. Turri,[16] W. Walkowiak,[16] D. C. Williams,[16] M. G. Wilson,[16]
E. Chen,[17] G. P. Dubois-Felsmann,[17] A. Dvoretskii,[17] D. G. Hitlin,[17] S. Metzler,[17] J. Oyang,[17] F. C. Porter,[17]
A. Ryd,[17] A. Samuel,[17] M. Weaver,[17] S. Yang,[17] R. Y. Zhu,[17] S. Devmal,[18] T. L. Geld,[18] S. Jayatilleke,[18]
G. Mancinelli,[18] B. T. Meadows,[18] M. D. Sokoloff,[18] T. Barillari,[19] P. Bloom,[19] M. O. Dima,[19] W. T. Ford,[19]
U. Nauenberg,[19] A. Olivas,[19] P. Rankin,[19] J. Roy,[19] J. G. Smith,[19] W. C. van Hoek,[19] J. Blouw,[20] J. L. Harton,[20]
M. Krishnamurthy,[20] A. Soffer,[20] W. H. Toki,[20] R. J. Wilson,[20] J. Zhang,[20] T. Brandt,[21] J. Brose,[21]
T. Colberg,[21] M. Dickopp,[21] R. S. Dubitzky,[21] A. Hauke,[21] E. Maly,[21] R. Muller-Pfefferkorn,[21] S. Otto,[21]
K. R. Schubert,[21] R. Schwierz,[21] B. Spaan,[21] L. Wilden,[21] D. Bernard,[22] G. R. Bonneaud,[22] F. Brochard,[22]
J. Cohen-Tanugi,[22] S. Ferrag,[22] S. T'Jampens,[22] Ch. Thiebaux,[22] G. Vasileiadis,[22] M. Verderi,[22] A. Anjomshoaa,[23]
R. Bernet,[23] A. Khan,[23] D. Lavin,[23] F. Muheim,[23] S. Playfer,[23] J. E. Swain,[23] J. Tinslay,[23] M. Falbo,[24]
C. Borean,[25] C. Bozzi,[25] S. Dittongo,[25] L. Piemontese,[25] E. Treadwell,[26] F. Anulli,[27] R. Baldini-Ferroli,[27]
A. Calcaterra,[27] R. de Sangro,[27] D. Falciai,[27] G. Finocchiaro,[27] P. Patteri,[27] I. M. Peruzzi,[27] M. Piccolo,[27]
Y. Xie,[27] A. Zallo,[27] S. Bagnasco,[28] A. Buzzo,[28] R. Contri,[28] G. Crosetti,[28] M. Lo Vetere,[28] M. Macri,[28]
M. R. Monge,[28] S. Passaggio,[28] F. C. Pastore,[28] C. Patrignani,[28] M. G. Pia,[28] E. Robutti,[28] A. Santroni,[28]
S. Tosi,[28] M. Morii,[29] R. Bartoldus,[30] R. Hamilton,[30] U. Mallik,[30] J. Cochran,[31] H. B. Crawley,[31] P.-A. Fischer,[31]
J. Lamsa,[31] W. T. Meyer,[31] E. I. Rosenberg,[31] G. Grosdidier,[32] C. Hast,[32] A. Hocker,[32] H. M. Lacker,[32]
S. Laplace,[32] V. Lepeltier,[32] A. M. Lutz,[32] S. Plaszczynski,[32] M. H. Schune,[32] S. Trincaz-Duvoid,[32] G. Wormser,[32]
R. M. Bionta,[33] V. Brigljevic,[33] D. J. Lange,[33] M. Mugge,[33] K. van Bibber,[33] D. M. Wright,[33] A. J. Bevan,[34]
J. R. Fry,[34] E. Gabathuler,[34] R. Gamet,[34] M. George,[34] M. Kay,[34] D. J. Payne,[34] R. J. Sloane,[34] C. Touramanis,[34]
M. L. Aspinwall,[35] D. A. Bowerman,[35] P. D. Dauncey,[35] U. Egede,[35] I. Eschrich,[35] N. J. W. Gunawardane,[35]
J. A. Nash,[35] P. Sanders,[35] D. Smith,[35] D. E. Azzopardi,[36] J. J. Back,[36] G. Bellodi,[36] P. Dixon,[36] P. F. Harrison,[36]
R. J. L. Potter,[36] H. W. Shorthouse,[36] P. Strother,[36] P. B. Vidal,[36] G. Cowan,[37] S. George,[37] M. G. Green,[37]
A. Kurup,[37] C. E. Marker,[37] P. McGrath,[37] T. R. McMahon,[37] S. Ricciardi,[37] F. Salvatore,[37] G. Vaitsas,[37]
D. Brown,[38] C. L. Davis,[38] J. Allison,[39] R. J. Barlow,[39] J. T. Boyd,[39] A. C. Forti,[39] J. Fullwood,[39] F. Jackson,[39]
G. D. Lafferty,[39] N. Savvas,[39] J. H. Weatherall,[39] J. C. Williams,[39] A. Farbin,[40] A. Jawahery,[40] V. Lillard,[40]
J. Olsen,[40] D. A. Roberts,[40] J. R. Schieck,[40] G. Blaylock,[41] C. Dallapiccola,[41] K. T. Flood,[41] S. S. Hertzbach,[41]
R. Kofler,[41] V. B. Koptchev,[41] T. B. Moore,[41] H. Staengle,[41] S. Willocq,[41] B. Brau,[42] R. Cowan,[42] G. Sciolla,[42]
F. Taylor,[42] R. K. Yamamoto,[42] M. Milek,[43] P. M. Patel,[43] F. Palombo,[44] J. M. Bauer,[45] L. Cremaldi,[45]
V. Eschenburg,[45] R. Kroeger,[45] J. Reidy,[45] D. A. Sanders,[45] D. J. Summers,[45] J. Y. Nief,[46] P. Taras,[46]

H. Nicholson,[47] C. Cartaro,[48] N. Cavallo,[48,y] G. De Nardo,[48] F. Fabozzi,[48] C. Gatto,[48] L. Lista,[48] P. Paolucci,[48]
D. Piccolo,[48] C. Sciacca,[48] J. M. LoSecco,[49] J. R. G. Alsmiller,[50] T. A. Gabriel,[50] J. Brau,[51] R. Frey,[51]
E. Grauges,[51] M. Iwasaki,[51] N. B. Sinev,[51] D. Strom,[51] F. Colecchia,[52] F. Dal Corso,[52] A. Dorigo,[52] F. Galeazzi,[52]
M. Margoni,[52] G. Michelon,[52] M. Morandin,[52] M. Posocco,[52] M. Rotondo,[52] F. Simonetto,[52] R. Stroili,[52]
E. Torassa,[52] C. Voci,[52] M. Benayoun,[53] H. Briand,[53] J. Chauveau,[53] P. David,[53] Ch. de la Vaissiere,[53] L. Del
Buono,[53] O. Hamon,[53] F. Le Diberder,[53] Ph. Leruste,[53] J. Ocariz,[53] L. Roos,[53] J. Stark,[53] P. F. Manfredi,[54]
V. Re,[54] V. Speziali,[54] E. D. Frank,[55] L. Gladney,[55] Q. H. Guo,[55] J. Panetta,[55] C. Angelini,[56] G. Batignani,[56]
S. Bettarini,[56] M. Bondioli,[56] F. Bucci,[56] E. Campagna,[56] M. Carpinelli,[56] F. Forti,[56] M. A. Giorgi,[56] A. Lusiani,[56]
G. Marchiori,[56] F. Martinez-Vidal,[56] M. Morganti,[56] N. Neri,[56] E. Paoloni,[56] M. Rama,[56] G. Rizzo,[56] F. Sandrelli,[56]
G. Simi,[56] G. Triggiani,[56] J. Walsh,[56] M. Haire,[57] D. Judd,[57] K. Paick,[57] L. Turnbull,[57] D. E. Wagoner,[57]
J. Albert,[58] P. Elmer,[58] C. Lu,[58] V. Miftakov,[58] S. F. Schaffner,[58] A. J. S. Smith,[58] A. Tumanov,[58] E. W. Varnes,[58]
G. Cavoto,[59] D. del Re,[59] R. Faccini,[14,59] F. Ferrarotto,[59] F. Ferroni,[59] E. Lamanna,[59] M. A. Mazzoni,[59]
S. Morganti,[59] G. Piredda,[59] F. Safai Tehrani,[59] M. Serra,[59] C. Voena,[59] S. Christ,[60] R. Waldi,[60] T. Adye,[61]
N. De Groot,[61] B. Franek,[61] N. I. Geddes,[61] G. P. Gopal,[61] S. M. Xella,[61] R. Aleksan,[62] S. Emery,[62]
A. Gaidot,[62] S. F. Ganzhur,[62] P.-F. Giraud,[62] G. Hamel de Monchenault,[62] W. Kozanecki,[62] M. Langer,[62]
G. W. London,[62] B. Mayer,[62] B. Serfass,[62] G. Vasseur,[62] Ch. Yeche,[62] M. Zito,[62] M. V. Purohit,[63] H. Singh,[63]
A. W. Weidemann,[63] F. X. Yumiceva,[63] I. Adam,[64] D. Aston,[64] N. Berger,[64] A. M. Boyarski,[64] G. Calderini,[64]
M. R. Convery,[64] D. P. Coupal,[64] D. Dong,[64] J. Dorfan,[64] W. Dunwoodie,[64] R. C. Field,[64] T. Glanzman,[64]
S. J. Gowdy,[64] T. Haas,[64] T. Himel,[64] T. Hryn'ova,[64] M. E. Huffer,[64] W. R. Innes,[64] C. P. Jessop,[64]
M. H. Kelsey,[64] P. Kim,[64] M. L. Kocian,[64] U. Langenegger,[64] D. W. G. S. Leith,[64] S. Luitz,[64] V. Luth,[64]
H. L. Lynch,[64] H. Marsiske,[64] S. Menke,[64] R. Messner,[64] D. R. Muller,[64] C. P. O'Grady,[64] V. E. Ozcan,[64]
A. Perazzo,[64] M. Perl,[64] S. Petrak,[64] H. Quinn,[64] B. N. Ratcliff,[64] S. H. Robertson,[64] A. Roodman,[64]
A. A. Salnikov,[64] T. Schietinger,[64] R. H. Schindler,[64] J. Schwiening,[64] A. Snyder,[64] A. Soha,[64] S. M. Spanier,[64]
J. Stelzer,[64] D. Su,[64] M. K. Sullivan,[64] H. A. Tanaka,[64] J. Va'vra,[64] S. R. Wagner,[64] A. J. R. Weinstein,[64]
W. J. Wisniewski,[64] D. H. Wright,[64] C. C. Young,[64] P. R. Burchat,[65] C. H. Cheng,[65] T. I. Meyer,[65] C. Roat,[65]
R. Henderson,[66] W. Bugg,[67] H. Cohn,[67] J. M. Izen,[68] I. Kitayama,[68] X. C. Lou,[68] F. Bianchi,[69] M. Bona,[69]
D. Gamba,[69] L. Bosisio,[70] G. Della Ricca,[70] L. Lanceri,[70] P. Poropat,[70] G. Vuagnin,[70] R. S. Panvini,[71]
C. M. Brown,[72] P. D. Jackson,[72] R. Kowalewski,[72] J. M. Roney,[72] H. R. Band,[73] E. Charles,[73] S. Dasu,[73]
A. M. Eichenbaum,[73] H. Hu,[73] J. R. Johnson,[73] R. Liu,[73] F. Di Lodovico,[73] Y. Pan,[73] R. Prepost,[73] I. J. Scott,[73]
S. J. Sekula,[73] J. H. von Wimmersperg-Toeller,[73] S. L. Wu,[73] Z. Yu,[73] T. M. B. Kordich,[74] and H. Neal[74]

(The BABAR Collaboration)

[1] Laboratoire de Physique des Particules, F-74941 Annecy-le-Vieux, France
[2] Universita di Bari, Dipartimento di Fisica and INFN, I-70126 Bari, Italy
[3] Institute of High Energy Physics, Beijing 100039, China
[4] University of Bergen, Inst. of Physics, N-5007 Bergen, Norway
[5] Lawrence Berkeley National Laboratory and University of California, Berkeley, CA 94720, USA
[6] University of Birmingham, Birmingham, B15 2TT, United Kingdom
[7] Ruhr Universitat Bochum, Institut fur Experimentalphysik 1, D-44780 Bochum, Germany
[8] University of Bristol, Bristol BS8 1TL, United Kingdom
[9] University of British Columbia, Vancouver, BC, Canada V6T 1Z1
[10] Brunel University, Uxbridge, Middlesex UB8 3PH, United Kingdom
[11] Budker Institute of Nuclear Physics, Novosibirsk 630090, Russia
[12] University of California at Irvine, Irvine, CA 92697, USA
[13] University of California at Los Angeles, Los Angeles, CA 90024, USA
[14] University of California at San Diego, La Jolla, CA 92093, USA
[15] University of California at Santa Barbara, Santa Barbara, CA 93106, USA
[16] University of California at Santa Cruz, Institute for Particle Physics, Santa Cruz, CA 95064, USA
[17] California Institute of Technology, Pasadena, CA 91125, USA
[18] University of Cincinnati, Cincinnati, OH 45221, USA
[19] University of Colorado, Boulder, CO 80309, USA
[20] Colorado State University, Fort Collins, CO 80523, USA
[21] Technische Universitat Dresden, Institut fur Kern- und Teilchenphysik, D-01062 Dresden, Germany
[22] Ecole Polytechnique, F-91128 Palaiseau, France
[23] University of Edinburgh, Edinburgh EH9 3JZ, United Kingdom
[24] Elon University, Elon University, NC 27244-2010, USA
[25] Universita di Ferrara, Dipartimento di Fisica and INFN, I-44100 Ferrara, Italy

[26]Florida A&M University, Tallahassee, FL 32307, USA
[27]Laboratori Nazionali di Frascati dell'INFN, I-00044 Frascati, Italy
[28]Universita di Genova, Dipartimento di Fisica and INFN, I-16146 Genova, Italy
[29]Harvard University, Cambridge, MA 02138, USA
[30]University of Iowa, Iowa City, IA 52242, USA
[31]Iowa State University, Ames, IA 50011-3160, USA
[32]Laboratoire de l'Accelerateur Lineaire, F-91898 Orsay, France
[33]Lawrence Livermore National Laboratory, Livermore, CA 94550, USA
[34]University of Liverpool, Liverpool L69 3BX, United Kingdom
[35]University of London, Imperial College, London, SW7 2BW, United Kingdom
[36]Queen Mary, University of London, E1 4NS, United Kingdom
[37]University of London, Royal Holloway and Bedford New College, Egham, Surrey TW20 0EX, United Kingdom
[38]University of Louisville, Louisville, KY 40292, USA
[39]University of Manchester, Manchester M13 9PL, United Kingdom
[40]University of Maryland, College Park, MD 20742, USA
[41]University of Massachusetts, Amherst, MA 01003, USA
[42]Massachusetts Institute of Technology, Laboratory for Nuclear Science, Cambridge, MA 02139, USA
[43]McGill University, Montreal, QC, Canada H3A 2T8
[44]Universita di Milano, Dipartimento di Fisica and INFN, I-20133 Milano, Italy
[45]University of Mississippi, University, MS 38677, USA
[46]Universite de Montreal, Laboratoire Rene J. A. Levesque, Montreal, QC, Canada H3C 3J7
[47]Mount Holyoke College, South Hadley, MA 01075, USA
[48]Universita di Napoli Federico II, Dipartimento di Scienze Fisiche and INFN, I-80126, Napoli, Italy
[49]University of Notre Dame, Notre Dame, IN 46556, USA
[50]Oak Ridge National Laboratory, Oak Ridge, TN 37831, USA
[51]University of Oregon, Eugene, OR 97403, USA
[52]Universita di Padova, Dipartimento di Fisica and INFN, I-35131 Padova, Italy
[53]Universites Paris VI et VII, Lab de Physique Nucleaire H. E., F-75252 Paris, France
[54]Universita di Pavia, Dipartimento di Elettronica and INFN, I-27100 Pavia, Italy
[55]University of Pennsylvania, Philadelphia, PA 19104, USA
[56]Universita di Pisa, Scuola Normale Superiore and INFN, I-56010 Pisa, Italy
[57]Prairie View A&M University, Prairie View, TX 77446, USA
[58]Princeton University, Princeton, NJ 08544, USA
[59]Universita di Roma La Sapienza, Dipartimento di Fisica and INFN, I-00185 Roma, Italy
[60]Universitat Rostock, D-18051 Rostock, Germany
[61]Rutherford Appleton Laboratory, Chilton, Didcot, Oxon, OX11 0QX, United Kingdom
[62]DAPNIA, Commissariat a l'Energie Atomique/Saclay, F-91191 Gif-sur-Yvette, France
[63]University of South Carolina, Columbia, SC 29208, USA
[64]Stanford Linear Accelerator Center, Stanford, CA 94309, USA
[65]Stanford University, Stanford, CA 94305-4060, USA
[66]TRIUMF, Vancouver, BC, Canada V6T 2A3
[67]University of Tennessee, Knoxville, TN 37996, USA
[68]University of Texas at Dallas, Richardson, TX 75083, USA
[69]Universita di Torino, Dipartimento di Fiscia Sperimentale and INFN, I-10125 Torino, Italy
[70]Universita di Trieste, Dipartimento di Fisica and INFN, I-34127 Trieste, Italy
[71]Vanderbilt University, Nashville, TN 37235, USA
[72]University of Victoria, Victoria, BC, Canada V8W 3P6
[73]University of Wisconsin, Madison, WI 53706, USA
[74]Yale University, New Haven, CT 06511, USA

(Dated: January 4, 2002)

We present results from a search for the flavor-changing neutral current decays $B \to K\ell^+\ell^-$ and $B \to K^*\ell^+\ell^-$, where $\ell^+\ell^-$ is either an e^+e^- or $\mu^+\mu^-$ pair. The data sample comprises 22.7×10^6 $\Upsilon(4S) \to B\overline{B}$ decays collected with the BABAR detector at the PEP-II B Factory. We obtain the 90% C.L. upper limits $\mathcal{B}(B \to K\ell^+\ell^-) < 0.50 \times 10^{-6}$ and $\mathcal{B}(B \to K^*\ell^+\ell^-) < 2.9 \times 10^{-6}$, close to Standard Model predictions for these branching fractions. We have also obtained limits on the lepton-family-violating decays $B \to Ke\mu$ and $B \to K^*e\mu$.

PACS numbers: 13.25.Hw, 13.20.He

The flavor-changing neutral current decays $B \to K\ell^+\ell^-$ and $B \to K^*(892)\ell^+\ell^-$, where ℓ is a charged lepton, are highly suppressed in the Standard Model, with branching fractions predicted to be of order 10^{-7}–10^{-6} [1, 2]. The dominant contributions arise at the one-loop level and are known as electroweak penguins.

Besides probing Standard Model loop effects, these rare decays are important because their rates and kinematic distributions are sensitive to new, heavy particles—such as those predicted by supersymmetric models—that can appear virtually in the loop [1, 2].

The Standard Model predictions for $B \to K^{(*)}\ell^+\ell^-$ include three main contributions: the electromagnetic (EM) penguin, the Z penguin, and the W^+W^- box diagram. Evidence for the EM penguin amplitude has been obtained from the observation of $B \to K^*\gamma$ and inclusive $B \to X_s\gamma$, where X_s is any hadronic system with strangeness [3, 4].

Calculations of decay rates for $B \to K^{(*)}\ell^+\ell^-$ based on the Standard Model have significant uncertainties due to strong interactions. For example, Ali et al. [1] predict $\mathcal{B}(B \to K\ell^+\ell^-) = (0.57^{+0.17}_{-0.10}) \times 10^{-6}$ for both e^+e^- and $\mu^+\mu^-$ final states, $\mathcal{B}(B \to K^*e^+e^-) = (2.3^{+0.7}_{-0.5}) \times 10^{-6}$, and $\mathcal{B}(B \to K^*\mu^+\mu^-) = (1.9^{+0.5}_{-0.4}) \times 10^{-6}$. The contribution of the EM penguin amplitude to $B \to K^*\ell^+\ell^-$ is particularly strong at low values of $m_{\ell^+\ell^-}$, giving a larger rate for $B \to K^*e^+e^-$ than for $B \to K^*\mu^+\mu^-$.

We search for the following decays: $B^+ \to K^+\ell^+\ell^-$, $B^0 \to K^0_S\ell^+\ell^-$, $B^+ \to K^{*+}\ell^+\ell^-$, and $B^0 \to K^{*0}\ell^+\ell^-$, where $K^{*0} \to K^+\pi^-$, $K^{*+} \to K^0_S\pi^+$, $K^0_S \to \pi^+\pi^-$, and ℓ is either an e or μ. We also search for the lepton-family-violating decays $B \to K^{(*)}e\mu$. Throughout this paper, charge-conjugate modes are implied.

The data used in the analysis were collected with the BABAR detector at the PEP-II storage ring at the Stanford Linear Accelerator Center during 1999–2000. We analyzed a 20.7 fb^{-1} data sample taken on the $\Upsilon(4S)$ resonance consisting of $(22.7 \pm 0.4) \times 10^6$ $\Upsilon(4S) \to B\overline{B}$ events.

This search relies primarily on the charged-particle tracking and particle-identification capabilities of the BABAR detector [5]. Charged particle tracking is provided by a five-layer silicon vertex tracker (SVT) and a 40-layer drift chamber (DCH). The DIRC, a Cherenkov ring-imaging particle-identification system, is used for charged hadron identification. Electrons are identified using the electromagnetic calorimeter (EMC), which comprises 6580 thallium-doped CsI crystals. These systems are mounted inside a 1.5 T solenoidal superconducting magnet. Muons are identified in the instrumented flux return (IFR), in which resistive plate chambers are interleaved with the iron plates of the magnet flux return.

We extract the signal using the kinematic variables $m_{ES} = \sqrt{E_b^{*2} - (\sum_i \mathbf{p}^*_i)^2}$ and $\Delta E = \sum_i \sqrt{m_i^2 + \mathbf{p}_i^{*2}} - E_b^*$, where E_b^* is the beam energy in the e^+e^- rest (c.m.) frame, $\mathbf{p}^*_i$ is the c.m. momentum of daughter particle i in the B meson candidate, and m_i is the mass of particle i. For signal events, m_{ES} peaks at the B meson mass with a resolution of about 2.5 MeV/c^2 and ΔE peaks near zero, indicating that the candidate system of particles has total energy consistent with the beam energy in the c.m. frame.

To prevent bias in the analysis, we optimized the event-selection criteria using Monte Carlo samples: we did not look at the data in the signal region or in the sidebands that were used to measure the background until these criteria were fixed. Signal efficiencies were determined using the Ali et al. model [1].

We select events that have at least four charged tracks, the ratio R_2 of the second and zeroth Fox-Wolfram moments [6] less than 0.5, and two oppositely charged leptons with momentum $p > 0.5$ (1.0) GeV/c for e (μ) candidates. Electron-positron pairs consistent with photon conversions in the detector material are vetoed. We require charged kaon candidates to be identified as kaons and the charged pion in $K^* \to K\pi$ not to be identified as a kaon. For $B \to K^*\ell^+\ell^-$, we require the mass of the $K\pi$ candidate to be within 75 MeV/c^2 of the mean $K^*(892)$ mass. K^0_S candidates are reconstructed from two oppositely charged tracks that form a good vertex displaced from the primary vertex by at least 1 mm.

The decays $B \to J/\psi(\to \ell^+\ell^-)K^{(*)}$ and $B \to \psi(2S)(\to \ell^+\ell^-)K^{(*)}$ have identical topologies to signal events. These backgrounds are suppressed by applying a veto in the ΔE vs. $m_{\ell^+\ell^-}$ plane (Fig. 1). This veto removes charmonium events not only with reconstructed $m_{\ell^+\ell^-}$ values near the nominal charmonium masses, but also events that lie further away in $m_{\ell^+\ell^-}$ due to photon radiation (more pronounced in electron channels) or track mismeasurement. Removing all of these events simplifies the description of the background shape. Charmonium events can, however, pass this veto if one of the leptons (typically a muon) and the kaon are misidentified as each other. If reassignment of particle types results in a dilepton mass consistent with the J/ψ or $\psi(2S)$ mass, the candidate is vetoed. There is also significant feed-up from $B \to J/\psi K$ and $B \to \psi(2S)K$ into $B \to K^*\ell^+\ell^-$, since energy lost due to bremsstrahlung in $B \to J/\psi K$ can be compensated for by including a random pion. If the $K\pi\ell^+\ell^-$ system in a $B \to K^*\ell^+\ell^-$ candidate is kinematically consistent with $B \to J/\psi(\to \ell^+\ell^-\gamma)K$, assuming that the photon (which is not directly observed) was radiated along the direction of either lepton, then the candidate is vetoed. Apart from the charmonium vetoes, we analyze the full $m_{\ell^+\ell^-}$ range.

Continuum background from non-resonant $e^+e^- \to q\overline{q}$ production is suppressed using a Fisher discriminant [7], a linear combination of the input variables with optimized coefficients. The variables are R_2; $\cos\theta_B$, the cosine of the angle between the B candidate and the beam axis in the c.m. frame; $\cos\theta_T$, the cosine of the angle between the thrust axis of the candidate B meson daughter particles and that of the rest of the particles in the c.m. frame; and $m_{K\ell}$, the invariant mass of the K-lepton system, where the lepton is selected according to its charge relative to the strangeness of the $K^{(*)}$. The variable $m_{K\ell}$ helps discriminate against background from

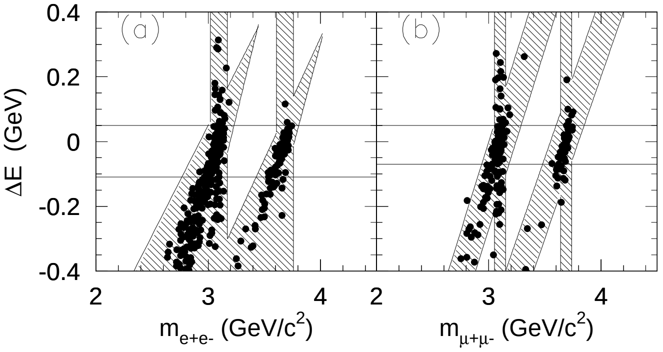

FIG. 1: Charmonium veto in the ΔE vs. $m_{\ell^+\ell^-}$ plane for (a) $B \to K^{(*)}e^+e^-$ and (b) $B \to K^{(*)}\mu^+\mu^-$. Hatched regions are vetoed. The dots correspond to a Monte Carlo simulation of $B \to J/\psi(\to \ell^+\ell^-)K$ and $B \to \psi(2S)(\to \ell^+\ell^-)K$. Most signal events would lie in the ΔE region between the horizontal lines.

semileptonic D decays, for which $m_{K\ell} < m_D$.

Combinatorial background from $B\bar{B}$ events is suppressed using a signal-to-$B\bar{B}$ likelihood ratio that combines candidate B and dilepton vertex probabilities; the significance of the dilepton separation along the beam direction; $\cos\theta_B$; and the missing energy, E_{miss}, of the event in the c.m. frame. The variable E_{miss} provides the strongest discrimination against $B\bar{B}$ background, since events with semileptonic decays usually have significant unobserved energy due to neutrinos. For each final state, we select at most one combination of particles per event as a B signal candidate. If multiple candidates occur, we select the candidate with the greatest number of drift chamber and SVT hits on the charged tracks.

We use the known charmonium decays $B \to J/\psi K^{(*)}$ and $B \to \psi(2S)K^{(*)}$ to check the efficiency of our analysis cuts. Figure 2 compares the ΔE distributions (absolutely normalized) of these charmonium samples in Monte Carlo with data. We find good agreement in both the normalization and the shape.

We extract the signal and background yields in each channel using a two-dimensional extended unbinned maximum likelihood fit in the region defined by $m_{ES} > 5.2$ GeV/c^2 and $|\Delta E| < 0.25$ GeV. The signal shapes, including the effects of radiation on the ΔE distribution and the correlation between m_{ES} and ΔE, are obtained by parametrizing the GEANT3 Monte Carlo [8] simulation of the signal. The background is described by a function [9] with two parameters that are determined in our fits to the data. Backgrounds from $B\bar{B}$ that peak in the signal region are suppressed to less than 0.2 events in each mode. Although we allow the signal yield to be negative, we have imposed a lower cut-off such that the total fit function is positive. The fit results are shown in Fig. 3 and summarized in Table I. We observe no significant signals.

To determine 90% C.L. upper limits on the signal yields, we generate and fit a series of toy Monte Carlo samples in which the background probability density function is taken from our fit to the data, but the mean number of signal events is varied. We generate ten thousand samples for each mean value, increasing the mean until 90% of the fits to a set of samples give a signal yield greater than that obtained by fitting the data. To give a measure of the sensitivity of the analysis we list in Table I an effective background yield. This quantity is defined as the square of the error on the signal yield from a fit to a toy Monte Carlo sample drawn from the background probability function, with no signal contribution.

Table I lists the systematic uncertainties from the fit, $(\Delta\mathcal{B}/\mathcal{B})_{fit}$, expressed according to their effect on the limits. The sensitivity of the limits to the values used for signal-shape parameters is determined by performing alternative fits using parameters from the $B \to J/\psi K^{(*)}$ control samples. For modes with electrons, we also varied the fraction of signal events in the tail of the ΔE distribution. To determine whether a more general background shape would lead to different results, we introduced additional parameters and allowed for a correlation between m_{ES} and ΔE. This procedure shifted the upper limits by 2% to 5%, depending on the mode. Most of the uncertainty associated with the background shape is incorporated in the statistical error on the yield because the background shape is determined from the fit.

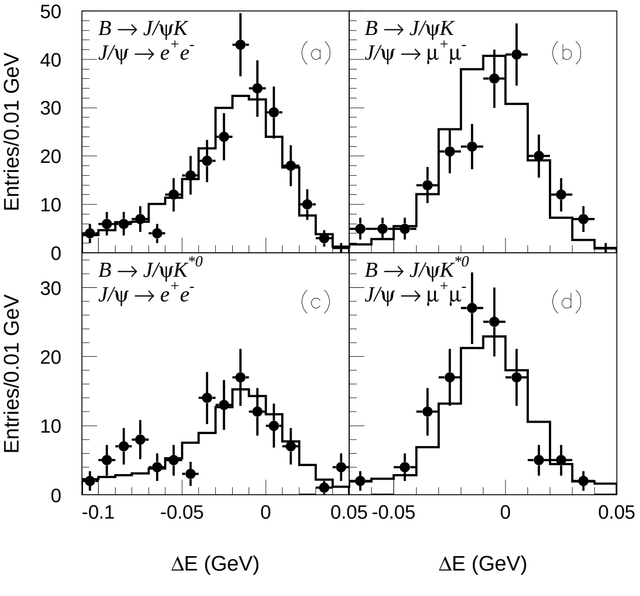

FIG. 2: Comparison of event yields and ΔE shapes between data and Monte Carlo for the charmonium control samples. The points with error bars show the data, and the solid histograms show the prediction of the charmonium Monte Carlo. All of the analysis selection criteria have been applied except for the charmonium veto, which is reversed. The large tails in the e^+e^- modes are due to photon radiation. Small shifts between data and Monte Carlo are taken into account as systematic uncertainties on the signal yields.

TABLE I: Results from the fits to $B \to K^{(*)}\ell^+\ell^-$ and $B \to K^{(*)}e\mu$ modes. The columns from left to right are fitted signal yield [10]; upper limit on the signal yield; the contribution of the background to the error on the signal yield, expressed as an effective background yield (see text); the signal efficiency, ϵ (not including the branching fractions for K^*, K^0, and K^0_S decays); the systematic error on the selection efficiency, $(\sigma_B/B)_\epsilon$; the systematic error from the fit, $(\sigma_B/B)_{\rm fit}$; the branching fraction central value (B); and the upper limit on the branching fraction, including systematic errors.

Mode	Signal yield	90% C.L. yield	Effective background	ϵ (%)	$(\sigma_B/B)_\epsilon$ (%)	$(\sigma_B/B)_{\rm fit}$ (%)	$B/10^{-6}$	$B/10^{-6}$ 90% C.L.
$B^+ \to K^+e^+e^-$	$0.2^{+1.5}_{-0.0}$	3.1	0.7	17.5	7.6	4.0	$0.0^{+0.4}_{-0.0}$	0.8
$B^+ \to K^+\mu^+\mu^-$	$0.3^{+1.3}_{-0.0}$	2.6	0.6	10.5	7.5	4.0	$0.1^{+0.5}_{-0.0}$	1.2
$B^0 \to K^{*0}e^+e^-$	$3.8^{+3.8}_{-2.1}$	8.8	1.4	10.2	8.8	11.9	$2.5^{+2.5}_{-1.4}$	6.6
$B^0 \to K^{*0}\mu^+\mu^-$	$0.3^{+1.7}_{-0.0}$	3.5	0.7	8.0	10.8	3.0	$0.2^{+1.4}_{-0.0}$	3.2
$B^0 \to K^0e^+e^-$	$1.1^{+2.7}_{-0.9}$	4.2	0.2	15.7	8.8	9.5	$0.9^{+2.2}_{-0.8}$	3.9
$B^0 \to K^0\mu^+\mu^-$	$0.0^{+1.2}_{-0.0}$	2.5	0.1	9.6	8.8	3.0	$0.0^{+1.6}_{-0.0}$	3.7
$B^+ \to K^{*+}e^+e^-$	$0.4^{+1.9}_{-0.0}$	3.8	1.6	8.5	11.0	5.0	$0.8^{+4.3}_{-0.0}$	9.6
$B^+ \to K^{*+}\mu^+\mu^-$	$1.2^{+2.4}_{-1.0}$	4.5	0.3	5.8	13.0	7.6	$3.9^{+8.1}_{-3.2}$	17.3
$B^+ \to K^+e\mu$	$0.4^{+1.4}_{-0.0}$	2.9	1.3	16.8	5.7	4.0	$0.1^{+0.4}_{-0.0}$	0.8
$B^0 \to K^{*0}e\mu$	$1.1^{+3.3}_{-1.6}$	5.3	2.7	11.9	7.1	10.4	$0.6^{+1.8}_{-0.9}$	3.3
$B^0 \to K^0e\mu$	$1.1^{+2.1}_{-0.9}$	4.1	0.5	14.6	7.3	11.2	$0.9^{+1.9}_{-0.8}$	4.1
$B^+ \to K^{*+}e\mu$	$0.4^{+1.8}_{-0.0}$	3.5	1.1	9.3	9.6	3.0	$0.8^{+3.8}_{-0.0}$	8.0

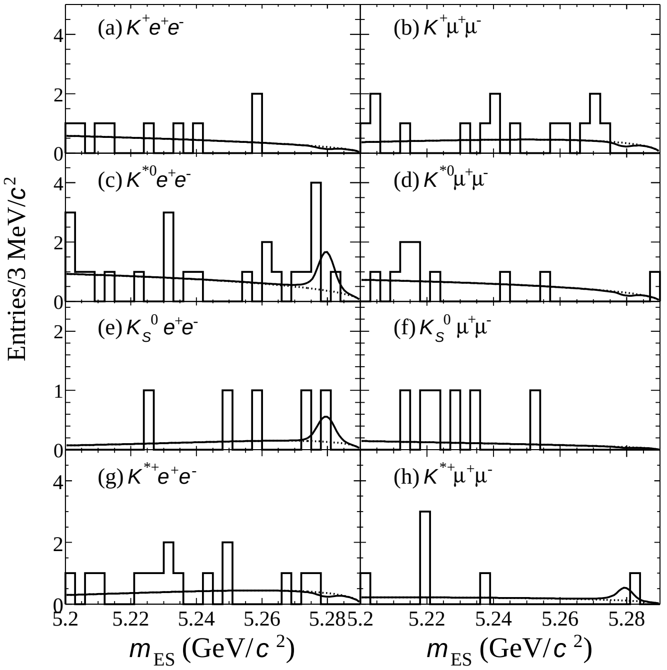

FIG. 3: Projections from individual maximum likelihood fits onto $m_{\rm ES}$ for the ΔE signal regions: $-0.11 < \Delta E < 0.05$ GeV (electrons) and $-0.07 < \Delta E < 0.05$ GeV (muons). The dotted lines show the background component, and the solid lines show the sum of background and signal components.

The systematic uncertainties on the efficiency, $(\sigma_B/B)_\epsilon$, are listed in Table I and arise from charged-particle tracking (1.2%/lepton, 2.0% for the pion from $K^* \to K\pi$, and 1.3%/track for other charged hadrons), particle identification (1.4%/electron, 1.0%/muon, 2.0%/track for kaons and pions), the continuum suppression cut (2.0%), the $B\overline{B}$ suppression cut (3.0%), K^0_S selection (4.0%), Monte Carlo signal statistics (3.0% to 5.0%), the theoretical model dependence of the efficiency (4.0% to 7.0%, depending on the mode), and the number of $B\overline{B}$ events (1.6%). The uncertainties on the efficiencies due to model-dependence of form factors are taken to be the full range of variation obtained from different theoretical models [1]. In setting an upper limit, the systematic uncertainties from the efficiency, $(\sigma_B/B)_\epsilon$, and from the fit, $(\sigma_B/B)_{\rm fit}$, are added in quadrature, and the limit is increased by this factor.

Table I also includes the results for the lepton-family-violating decays $B \to K^{(*)}e\mu$, where the signal efficiencies were determined from phase-space Monte Carlo simulations. We observe no evidence for these decays.

We determine the branching fractions $\mathcal{B}(B \to K\ell^+\ell^-)$ and $\mathcal{B}(B \to K^*\ell^+\ell^-)$ averaged over both B meson charge and lepton type (e^+e^- and $\mu^+\mu^-$) by performing a simultaneous maximum likelihood fit to the four contributing channels in each case. In combining the $B \to K^*\ell^+\ell^-$ modes, the ratio of branching fractions $\mathcal{B}(B \to K^*e^+e^-)/\mathcal{B}(B \to K^*\mu^+\mu^-) = 1.2$ from the model of Ali et al. [1] is used to weight the yield in the muon channel relative to that in the electron channel. The extracted yield corresponds to the electron mode. The combined fits give

$$\mathcal{B}(B \to K\ell^+\ell^-) = (0.06^{+0.24}_{-0.00} \pm 0.03) \times 10^{-6};$$

$$\mathcal{B}(B \to K^*\ell^+\ell^-) = (0.9^{+1.3}_{-0.9} \pm 0.1) \times 10^{-6};$$

where the first error is statistical and the second is systematic. We evaluate the upper limits on these combined modes and obtain

$$\mathcal{B}(B \to K\ell^+\ell^-) < 0.50 \times 10^{-6} \text{ at 90\% C.L.}$$

$$\mathcal{B}(B \to K^*\ell^+\ell^-) < 2.9 \times 10^{-6} \text{ at 90\% C.L.}$$

These limits represent an improvement over previously published results from CDF [11] and CLEO [12]. The Belle [13] experiment has also recently obtained results on these modes. We see no evidence for a signal, and our limits are close to many of the predictions based on the Standard Model. With the rapidly increasing size of our data sample, we expect to have significantly better sensitivity to these modes in the future.

We are grateful for the excellent luminosity and machine conditions provided by our PEP-II colleagues. The collaborating institutions wish to thank SLAC for its support and kind hospitality. This work is supported by DOE and NSF (USA), NSERC (Canada), IHEP (China), CEA and CNRS-IN2P3 (France), BMBF (Germany), INFN (Italy), NFR (Norway), MIST (Russia), and PPARC (United Kingdom). Individuals have received support from the Swiss NSF, A. P. Sloan Foundation, Research Corporation, and Alexander von Humboldt Foundation.

Also with Universita di Perugia, Perugia, Italy

† Also with Universita della Basilicata, Potenza, Italy

[1] A. Ali et al., Phys. Rev. D 61, 074024 (2000); P. Colangelo et al., Phys. Rev. D 53, 3672 (1996); D. Melikhov, N. Nikitin, and S. Simula, Phys. Rev. D 57, 6814 (1998).

[2] T.M. Aliev et al., Phys. Lett. B 400, 194 (1997); T.M. Aliev, M. Savci, and A. Özpineci, Phys. Rev. D 56, 4260 (1997); G. Burdman, Phys. Rev. D 52, 6400 (1995); C. Greub, A. Ioannissian, and D. Wyler, Phys. Lett. B 346, 149 (1995); J.L. Hewett and J.D. Wells, Phys. Rev. D 55, 5549 (1997); C.Q. Geng and C.P. Kao, Phys. Rev. D 54, 5636 (1996); and references therein.

[3] CLEO Collaboration, R. Ammar et al., Phys. Rev. Lett. 71, 674 (1993).

[4] CLEO Collaboration, M.S. Alam et al., Phys. Rev. Lett. 74, 2885 (1995).

[5] BABAR Collaboration, B. Aubert et al., hep-ex/0105044, to appear in Nucl. Instrum. Methods (2001).

[6] G.C. Fox and S. Wolfram, Phys. Rev. Lett. 41, 1581 (1978).

[7] R.A. Fisher, Ann. Eugenics 7, 179 (1936).

[8] “GEANT – Detector Description and Simulation Tool”, CERN Program Library Long Writeup W5013 (1995).

[9] We parametrize the background shape using

$$f(m_{ES}; E) = N e^{sE} m_{ES} \sqrt{1 \frac{m_{ES}^2}{E_b^2}} e^{1 \frac{m_{ES}^2}{E_b^2}} ;$$

where N is a normalization factor and s and are free parameters determined from the fit to the data.

[10] Whenever possible, we report two-sided 68% central confidence intervals. For channels constrained by the requirement that the total fit function be non-negative, we quote a single-sided 68% confidence interval and set the lower statistical error to zero.

[11] CDF Collaboration, T. Affolder et al., Phys. Rev. Lett. 83, 3378 (1999).

[12] CLEO Collaboration, S. Anderson et al., Phys. Rev. Lett. 87, 181803 (2001).

[13] Belle Collaboration, K. Abe et al., hep-ex/0109026, submitted to Phys. Rev. Lett.